ELSEVIER

Wear 181–183 (1995) 241–249

WEAR

Wear mechanisms of UHMWPE in total joint replacements

A. Wang, D.C. Sun, C. Stark, J.H. Dumbleton

Howmedica Inc. Division of Pfizer Hospital Products Group, Rutherford, NJ, USA

Abstract

The wear of ultra-high molecular weight polyethylene (UHMWPE) has become a major focus regarding the long-term clinical performance of total joint replacements. Clinical retrieval analysis has revealed the existence of two distinct wear mechanisms that are operational in both total hip and total knee replacements. While the majority of the wear debris produced from the acetabular component is less than a micron in size and often particulate or fibrous in shape, much larger thin flake-like wear debris is produced from the tibial component. Two theoretical wear models that are based on the scale of intimate asperity interactions are proposed to account for the observed differences in hip and knee wear. Cyclic plastic strain accumulation is identified as the common cause for wear debris generation in both hip and knee replacements. In the case of acetabular cup wear, the scale of plastic deformation is limited to the sites of intimate micro-asperity contacts and the wear rate is defined by a critical strain criterion. In the case of tibial component wear, however, plastic deformation spreads into the subsurface to the site of macro-asperity contacts, and material can be removed by subsurface cracking and delamination. In both cases, the wear rate is strongly affected by the ultimate tensile strength and breaking elongation of the UHMWPE material.

Keywords: UHMWPE; Total joint replacements; Strain accumulation

1. Introduction

Ultra-high molecular weight polyethylene (UHMWPE) has been the choice of orthopaedic bearing material in total joint replacements for the past twenty years. It has become more and more evident that the wear of UHMWPE may be the limiting factor that compromises the long-term performance of joint prostheses [1–5]. Clinical studies have found that loosening and failure in total hip replacement can be closely associated with osteolysis and bone resportion that are induced by fine polyethylene particles [1,3]. In total knee replacement, however, loosening and failure are often associated with excessive wear of the UHMWPE component that results in mechanical malfunctioning of the prosthesis [4,5]. Studies on clinically retrieved components and bone tissues have revealed that the majority of the wear debris produced in a total hip replacement is less than a micron in size and often particulate or fibrous in shape [6]. The most severe form of knee wear is, however, identified as pitting and delamination that can produce wear debris of a much larger scale [7]. The differences in wear mechanisms between hip and knee are attributed to the difference in loading configurations that create distinct stress patterns within the acetabular and the tibial component. Linear elastic stress analysis using finite element methods [8] has shown that while the maximum principal stress within the UHMWPE during normal walking is usually less than 10 MPa for a total hip replacement, it can reach as high as 45 MPa for a total knee replacement. The latter value is beyond the yield strength of the UHMWPE (~ 20–25 MPa). Perhaps more importantly, the maximum shear stress occurs at the surface of the polyethylene component for the hip but in the subsurface for the knee. It is this subsurface shear stress component that is found to be directly responsible for pitting and delamination of the UHMWPE tibial component.

However, recent advances in linear elastic stress analysis have not led to any significant understanding of the wear mechanisms in UHMWPE in total joint replacements. This may be attributed to the fact that the wear of UHMWPE is not an elastic process in either the hip or the knee component. Studies on retrieved UHMWPE components using thin section cross polarized microscopy have revealed the existence of large amounts of residual plastic strain within the surface region of acetabular components [4,9,10]. Cold flow which is associated with permanent plastic deformation is often observed on clinically retrieved UHMWPE tibial components [4,5,11]. In this paper,

SSDI 0043-1648(94)07027-X

the two distinct wear mechanisms observed for hip and knee components are studied both theoretically and experimentally. The primary objective is to reveal the relationships between mechanical properties and wear rate for UHMWPE in total hip and total knee replacement.

2. Theoretical modeling

2.1. Microscopic wear model

When two engineering surfaces come into contact, plastic deformation normally occurs at the tips of intimate asperity contacts within the softer material. Depending on the magnitude of the applied load, plastic deformation may or may not spread into the bulk of the softer material. Figs. 1(a) and 1(b) illustrate schematically these two contact situations. In the case of Fig. 1(a), i.e. an acetabular cup/femoral head contact, only the microscopic asperities are plastically deformed while the the overall or nominal contact is elastic. During walking or articulation, every contact asperity on the UHMWPE surface will experience repeated cyclic deformation by the passing asperities on the femoral head. An incremental residual plastic strain, $\delta\epsilon$, is built into each unit contact spot with every encounter from the passing asperities on the counterface. Failure will occur when the ductility of material within each unit contact spot is exhausted. Therefore, this wear process can be modelled by a critical strain criterion. Assuming ϵ_c as the critical strain for the UHMWPE under the wear conditions, a wear particle may be produced when the accumulated plastic strain after n_c asperity encounters reaches the critical strain, i.e. when:

$$\delta\epsilon n_c = \epsilon_c \tag{1}$$

For simplicity, let us assume a fully plastic asperity contact situation and a uniform distribution of N asperities with equal height and equal tip radius on the femoral head within the apparent contact area. According to the random-walk theory [12], there will be N contact spots at any given moment and $N^{1/2}$ asperity passes sweeping through the same spot per walking cycle. During each walking cycle, these N asperities will sweep through a linear distance l_o over which a true contact area A_s will be covered. According to Fig. 2, A_s is given by:

$$A_s = 2al_oN^{1/2} \tag{2}$$

where a is the average radius of each unit contact spot as illustrated in Fig. 3. The total number of non-overlapping contact spots within A_s is given by:

$$N_o = \frac{A_s}{\pi a^2} = \frac{2l_o}{\pi a} N^{1/2} \tag{3}$$

The total number of wear particles produced within A_s per walking cycle is given by:

$$N_p = \frac{N^{1/2}}{n_c} N_o \tag{4}$$

Assuming that the volume of each wear particle produced is proportional to the deformed volume of the unit contact spot, i.e. $\delta v \propto a^3$, then the total volume of wear particles produced per walking cycle is:

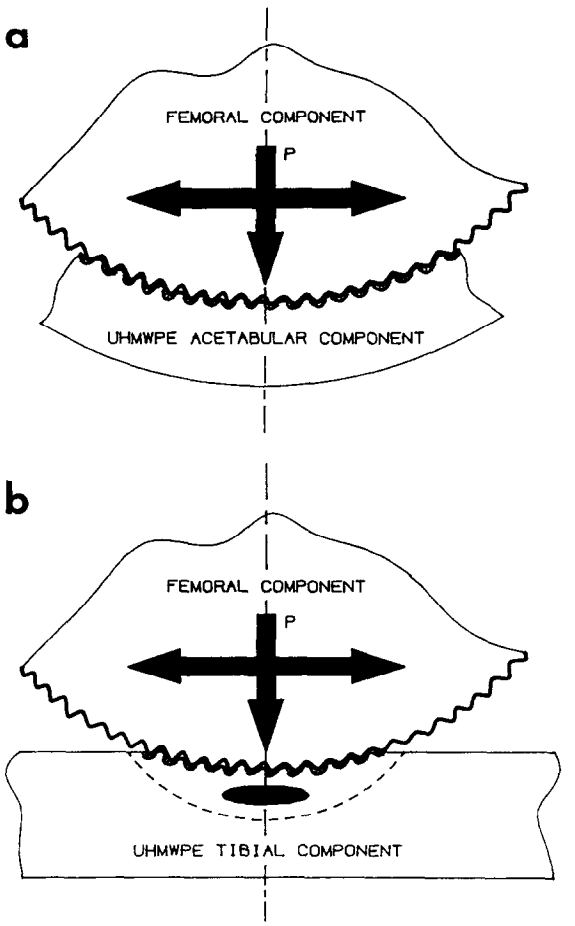

Fig. 1. Schematic illustrations of (a) a hip contact in which plastic deformation is limited to the micro-scale surface asperities and (b) a knee contact in which both the surface asperities and the nominal contact surface are plastically deformed. The scale of the surface asperities is exaggerated.

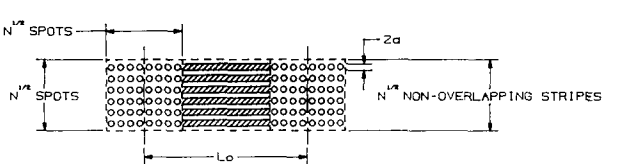

Fig. 2. Schematic illustration of the non-overlapping area that is swept by the surface asperities on the counterface at a sliding distance l_o. Assuming all asperities within the nominal contact area have equal height and equal tip radius.

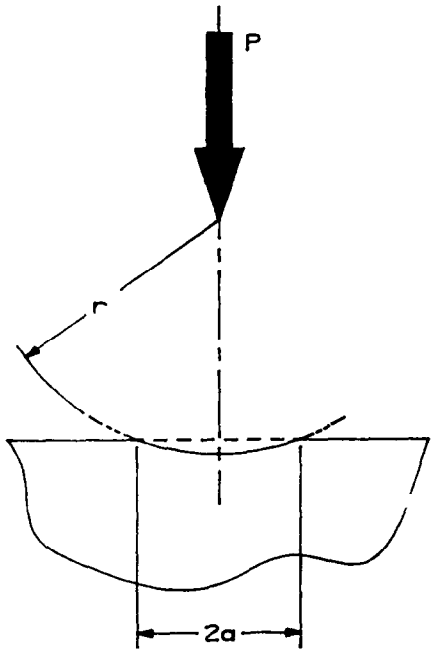

Fig. 3. Schematic illustration of the indentation of a perfectly flat half-space by a rigid spherical indenter.

$$\Delta V \alpha a^3 \frac{N^{1/2}}{n_c} N_o \tag{5}$$

Denoting P as the average applied load per walking cycle, p_o as the mean contact pressure within each unit asperity contact spot, then for fully plastic contact, p_o is roughly proportional to the flow stress, ρ_y, of the softer material [13], that is

$$p_o = \frac{P}{N\pi a^2} \alpha \rho_y \tag{6}$$

The average strain introduced into the contact spot per asperity pass is given by [13,14]

$$\delta\epsilon \alpha \frac{a}{r} \tag{7}$$

Substituting Eqs. (1), (3), (6) and (7) into Eqs. (4) and (5) yields:

$$N_p \alpha \frac{N}{r\epsilon_c} \tag{8}$$

and

$$\Delta V \alpha \left(\frac{P}{\rho_y}\right)^{3/2} \frac{1}{\epsilon_c r N^{1/2}} \tag{9}$$

Denote h as the average asperity height, for engineering surfaces it has been found experimentally that $N \alpha h^{-2}$ or $N^{1/2} \alpha h^{-1}$ [15]. Taking this relationship into Eqs. (8) and (9) yields:

$$N_p \alpha \frac{1}{\epsilon_c r h^2} \tag{10}$$

and

$$\Delta V \alpha \left(\frac{P}{\rho_y}\right)^{3/2} \frac{h}{r} \frac{1}{\epsilon_c} \tag{11}$$

Hollander and Lancaster [16] have found that for engineering surfaces h/r is approximately proportional to $R_a^{3/2}$. Therefore, Eqs. (10) and (11) may also be written as

$$N_p \alpha \frac{1}{\epsilon_c r^3 R_a^3} \tag{12}$$

and

$$\Delta V \alpha P^{3/2} R_a^{3/2} \frac{1}{\rho_y^{3/2} \epsilon_c} \tag{13}$$

where R_a is the center-line-average roughness value of the femoral head surface, r the average tip radius of the asperities, P the applied load, ρ_y the average flow stress and ϵ_c the critical strain of the UHMWPE. Due to strain hardening, the average flow stress ρ_y may approach the ultimate tensile strength of the UHMWPE. To a first approximation, one may substitute ρ_y and ϵ_c with the ultimate tensile strength σ_u and elongation at break ϵ_u as obtained in a tensile test. By doing so, Eq. (13) becomes:

$$\Delta V \alpha P^{3/2} R_a^{3/2} \frac{1}{\sigma_u^{3/2} \epsilon_u} \tag{14}$$

This relationship, i.e. $\Delta V \alpha \sigma_u^{-3/2} \epsilon_u^{-1}$, resembles the well-known Ratner–Lancaster experimental correlation [17] between abrasive wear and mechanical properties for polymers, i.e. $\Delta V \alpha (\sigma_u \epsilon_u)^{-1}$. Since $(\sigma_u \epsilon_u)$ represents the strain energy at break in a tensile test, both the present and the Ratner–Lancaster correlations imply that the tensile rupture energy or toughness of UHMWPE is the most important property that determines the volumetric wear rate.

2.2. Macroscopic wear model

While plastic deformation is limited to the sites of intimate micro-asperity contacts in acetabular cups, plastic deformation can spread into a much larger macroscopic scale in tibial components during normal articulation, Fig. 1(b). In the latter case, the macroscopic plastic deformation will be initiated at the subsurface to the point of contact where the principal shear stress is a maximum. Therefore, shear cracks could be initiated at the subsurface by cyclic deformation. Material could be removed from the UHMWPE component when these shear cracks develop into a macro-crack that propagates to the free surface. This wear process or delamination has been identified as the most severe wear mechanism that occurs in the UHMWPE tibial components [4,5,7,8].

The concept and phonomenon of delamination were first proposed by Suh et al [18] in the study of dry sliding wear of ductile metals. These researchers have shown that in dry or poorly lubricated sliding under heavy load the wear particles take the form of thin flakes. This process of 'delamination' occurs by cracks which initiate from inclusions in the severely strained material and propagate parallel to the surface. Following the observation of delamination wear, some attempts [19,20] were made to apply elastic fracture mechanics to the problem. These gave rather disapointing results on account of the high compressive stresses beneath a sliding contact which virtually suppresses mode I stress intensities, and severely attenuate mode II stress intensities through the action of friction between the crack faces. A more promising approach follows from the hypothesis that delamination cracks are ductile (plastic) shear fractures, formed by the linking of voids along planes of high shear. Teirlink et al. [21] have shown that a superimposed hydrostatic compression facilitates fracture in shear by suppressing the dilatation of voids which would otherwise lead to tensile failure. Johnson [22] has further emphasized that it is a characteristic of ductile fracture that the development of micro-cracks and voids into a macro-crack is a function of plastic strain rather than stress intensity at the tip of the crack.

Since the delamination of UHMWPE is a plastic strain driven fatigue process, it may be simulated by a low-cycle fatigue mechanism. Supposing that during each reciprocating cycle of a wear test or in a knee joint, the material at the maximum shear stress location, i.e. the subsurface, experiences an inelastic strain amplitude of $\Delta\epsilon_p$, the cyclic fatigue life of the material N may be related to $\Delta\epsilon_p$ by the Coffin–Manson Eq. [23], i.e.

$$N^{\alpha}=\frac{\epsilon_u}{\Delta\epsilon_p} \tag{15}$$

where α is a material constant which can be determined by a low-cycle fatigue test, ϵ_u is the elongation at break as obtained in a tensile test. Denoting ΔV as the wear rate (volume loss/cycle), then it shall be inversely proportional to N, i.e.

$$\Delta V \propto \frac{1}{N}=\left(\frac{\Delta\epsilon_p}{\epsilon_u}\right)^{\frac{1}{\alpha}} \tag{16}$$

It should be emphasized here that $\Delta\epsilon_p$ is the cyclic plastic strain range per reciprocating or articulating cycle. For a given contact stress range or applied load, $\Delta\epsilon_p$ will be a function of the material properties under cyclic loading conditions. For example, $\Delta\epsilon_p$ may be strongly influenced by the size and shape of its hysteresis loops obtained in a cyclic stress–strain test. It may also be strongly affected by the strain-hardening ability of the material and the flow stress. For semi-crystalline polymers, the constant α is usually between 0.25 and 0.5 [24]. Therefore, the ductility of the UHMWPE will have a very strong effect on the wear rate when delamination is the predominant wear mechanism.

Before delamination could take place, wear of UHMWPE tibial components will be limited to the surfaces of intimate asperity contacts. In this case, the model proposed for the acetabular cup wear may apply.

3. Experimental work

3.1. Materials and methods

A reciprocating cylinder-on-flat wear experiment was conducted to test the validity of the models proposed in the previous section. In order to cover a wide range of mechanical properties for the UHMWPE materials tested, both wear and tensile test specimens were machined from a UHMWPE rod stock (Poly-Hi annealed GUR415) and were irradiated in different atmospheres and then artificially aged to various degrees. Tensile tests were conducted according to ASTM standard D638. Table 1 summarizes the tensile test results (engineering stress and engineering strain) for each group of specimens prepared.

Wear tests were performed using three multi-station reciprocating ring-on-flat wear machines. Fig. 4 shows schematically the loading configuration of the specimen setup. The wear machines consist of thirty two individual specimen chambers which are connected to thirty two individual reservoirs each containing 300 ml diluted serum solution (30 vol.% serum + 70 vol.% deionized water + 0.2 wt.% sodium azide, serum purchased from Sigma Inc.) and a soak control specimen. During the test, the serum solutions were circulated constantly between specimen chambers and reservoirs so that the test temperature was always equal to the ambient temperature of 21 °C. Each of the rectangular UHMWPE specimens (19 mm long × 12.7 mm wide × 13 mm high) was loaded against a cast CoCr wheel which oscillated around a 60° arc for each oscillation cycle. The diameter of the CoCr wheel was 71.9 mm and the width was 25.4 mm. Since the wheels were twice as wide as the polymer specimens, edge contact was eliminated. All the wheels were highly polished and passivated. The average surface finish of the wheels was 0.05 μm (R_a). The applied load on each specimen was 250 lbs (1100 N) which gave rise to a maximum Hertzian contact pressure of $\approx$3000 psi ($\approx$20 MPa) at the start of test. At weekly intervals, all test and soak-control specimens were taken out of the test chambers, cleaned, dried and weighed to an accuracy of 0.01 mg. The test chambers and reservoirs were also cleaned and filled with fresh serum solutions. Then the test continued

Table 1
Tensile test results

Specimen group	Tensile yield strength (MPa)	Ultimate tensile strength (MPa)	Elongation-at-break (%)
A	26	60	380
B	24	39	277
C	23	49	339
D	25	49	300
E	x	21	[a]
F	x	25	[a]
G	28	31	169
H	26	40	337
I	25	52	380
J	26	40	338
K	24	46	325

[a] specimens showed no ductility.

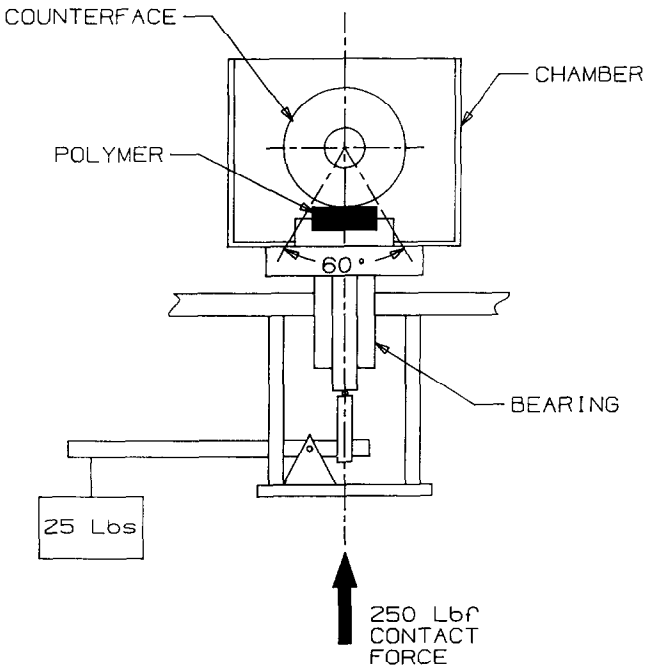

Fig. 4. Schematic of the loading configuration for the multi-station reciprocating ring-on-flat wear machines.

until five million cycles were reached. [1] Three specimens for each group were tested. All polymer specimens were presoaked in the same serum solution at room temperature for six weeks prior to wear testing.

Some of the wear specimens were photographed periodically at different test intervals. At the end of the test, some of the specimens were gold coated and examined by a scanning electron microscope (Phillips XL 40).

3.2. Experimental results

In general, most specimens showed a linear relationship between wear and number of cycles except groups E and F for which the initial wear rates were more than an order of magnitude higher than the steady-state wear rates. Figs. 5(a)–5(d) show the average volume loss for each group as a function of the number of cycles. Linear regression of the steady-state portion of the wear curves yields the steady-state wear rates for all groups of specimens. The data are shown in Table 2. Figs. 6(a)–6(c) show the plots of the steady-state wear rates as a function of the mechanical properties for all groups of specimens tested. In general, the wear rate is seen to increase with increasing the tensile yield strength but to decrease with increasing the ultimate tensile strength and breaking elongation. When plotted against the reciprocal of $\sigma_u^{3/2}\epsilon_u$ in Fig. 6(d), the wear rate shows an excellent linear relationship with these properties, supporting the theoretical prediction of the microscopic wear model.

Scanning electron micrographs of the worn surfaces of the specimens revealed two distinct morphologies for various groups of specimens. For those whose ul-

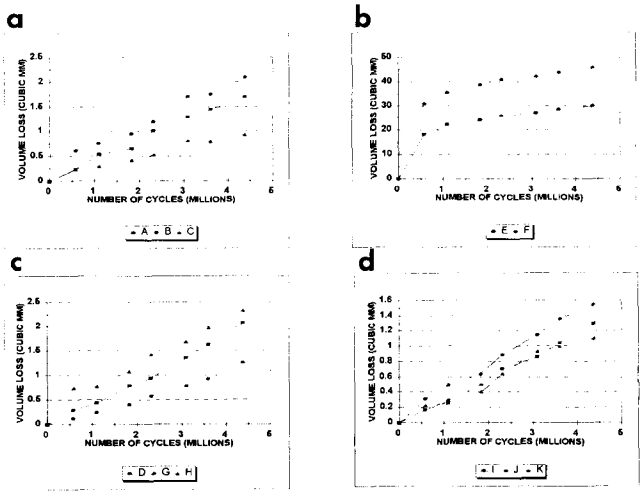

Fig. 5. Volume losses of UHMWPE as a function of the number of cycles: (a) Groups (A, B, C), (b) Groups (E, F), (c) Groups (D, G, H) and (d) Groups (I, J, K).

[1] Some of the specimens were run for shorter durations.

Table 2
Steady-state wear rates (mm^3 per million cycles)

Group	Wear rate (mm^3 10^{-6} cycles)	Standard deviation (STDS)	$\sigma_u^{-3/2}\epsilon_u^{-1}$ ($MPa^{-3/2}$)
A	0.225	0.043	5.662E−4
B	0.488	0.031	1.482E−3
C	0.239	0.055	1.05E−3
D	0.419	0.075	9.718E−4
E	4.421	1.605	[a]
F	3.351	0.538	[a]
G	0.652	0.055	3.43E−3
H	0.399	0.126	1.17E−3
I	0.286	0.060	7.02E−4
J	0.357	0.053	1.169−3
K	0.299	0.081	9.86E−4

[a] specimens showed no ductility.

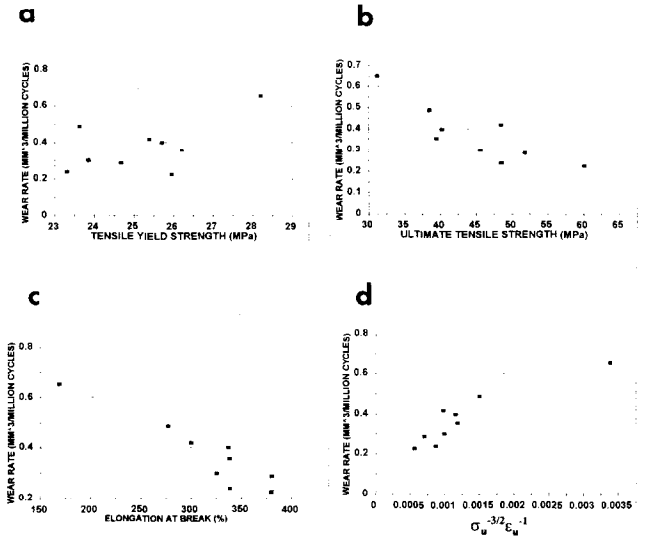

Fig. 6. Steady-state wear rates as a function of mechanical properties: (a) wear rate vs. tensile yield strength, (b) wear rate vs. ultimate tensile strength, (c) wear rate vs. elongation at break and (d) wear rate vs. $\sigma_u^{-3/2}$ ϵ_u^{-1}.

timate tensile strength values are greater than 32 MPa and breaking elongations are greater than 200%, the worn surfaces are smooth and almost featureless under very low magnifications, Fig. 7(a). At very high magnifications, a fine ripple-like appearance was observed, Fig. 7(b). The average inter-ripple spacing is less than a micron. It is well known in the erosion of ductile metals by solid particles that ripples are formed by a plastic strain accumulation process [25,26]. A similar process may be occurring in the wear of the UHMWPE specimens under the present experimental conditions. The micro-scale of the inter-ripple spacing may reflect the micro-nature of asperity contacts. Therefore, the micro-wear model proposed earlier is further strengthened by these observations.

Specimens in Groups E and F exhibited gross destruction to the surfaces, Figs. 8(a) and 8(b). During

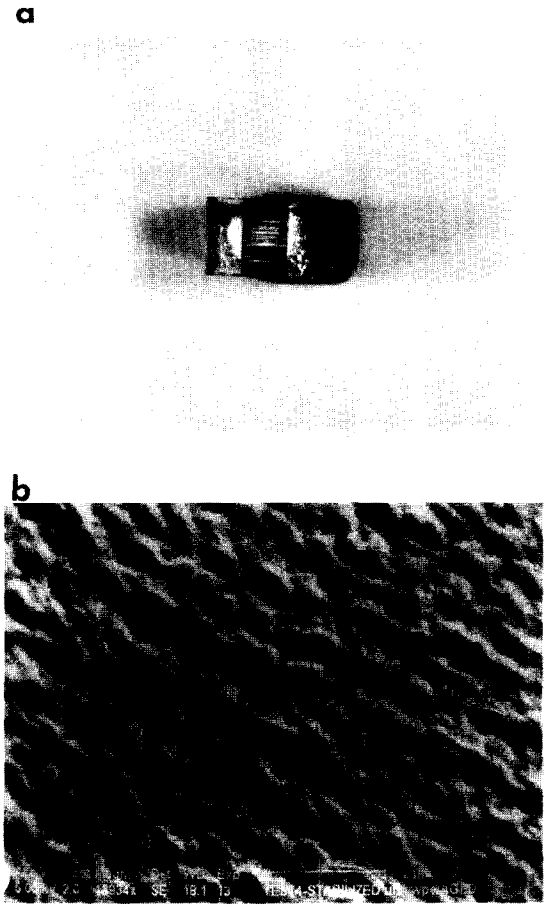

Fig. 7. Worn surface morphologies of a Group D specimen after 5 million cycles, (a) low magnification photograph and (b) high magnification scanning electron micrograph.

the initial high wear stage of articulation, massive wear debris at the scale of mm was produced by subsurface cracking and delamination, Fig. 8(b). This subsurface wear process gradually gave way to a surface wear process as the test proceeded to the steady-state during which the contact between the UHMWPE specimen

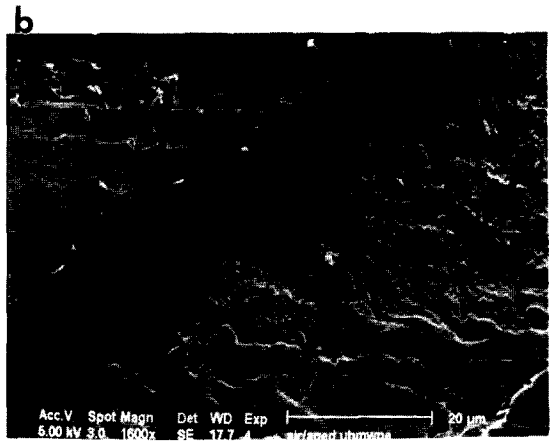

Fig. 8. Worn surface morphologies of a Group E specimen after 0.25 million cycles, (a) low magnification photograph and (b) high magnification scanning electron micrograph.

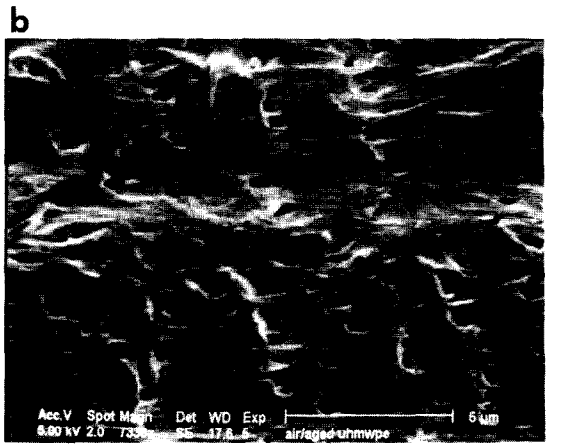

Fig. 9. Worn surface morphologies of a Group E specimen after 5 million cycles, (a) low magnification photograph and (b) high magnification scanning electron micrograph.

and the CoCr ring became conformal and the maximum shear stress moved to the surface. During the steady-state articulation, the worn surface became relatively smoother, Fig. 9(a). However, micro-cracking took place at the surface, Fig. 9(b). Most of the surface cracks were bridged by fibrils. Those fibrils could be the potential source for fibrous like wear debris as sometimes observed in the wear of acctabular cups. Clearly, this transition from subsurface wear to surface wear accounts for the transition in wear rate observed for Groups E and F whose ultimate tensile strength values are below 30 MPa and ductility almost equals to 0.

4. Discussion

The experimental results presented in the previous section have revealed the existence of both a microscopic surface wear process and a macroscopic subsurface wear process for UHMWPE. Under a given loading condition, the transition between these two wear processes depends critically upon the mechanical properties of the UHMWPE. The ultimate tensile strength and breaking elongation seem to be the most important material properties that determine the occurance of such a transition. Although the contact geometry is non-conformal for this particular experimental setup, the predominant wear mechanisms were microscopic surface wear and were not affected by the existence of a subsurface shear stress maximum unless the ultimate tensile strength and ductility of the UHMWPE specimens were significantly reduced. Therefore, this particular test method is as much a hip test method rather than a knee test method. More extreme conditions are needed in order to test for knee-type wear mechanisms. This work is on-going and will be published in the future.

As far as the microscopic surface wear is concerned, the ultimate tensile strength and breaking elongation are the most important material properties that determine the wear rate for UHMWPE. The experimental results not only support the present microscopic wear model but also confirm the well-known Ratner–Lancaster experimental correlation between abrasive wear and mechanical properties for polymers [17].

Therefore, in order to enhance the wear resistance for UHMWPE orthopaedic bearing materials, the ultimate tensile strength and ductility or toughness must be improved. Increases in the tensile yield strength are usually achieved at the expense of the toughness of the UHMWPE. Therefore, "enhancement" of the yield strength may well lead to an increased wear rate for the UHMWPE due to a reduction in toughness.

The microscopic wear model also reveals a strong dependence of wear rate on the applied load and surface roughness of the counterface. Eq. (14) predicts that the wear rate should be proportional to the 3/2th power of load. It was found experimentally by Rose and Cimino [27] that the wear rate of high density polyethylene under serum lubricated conditions increases non-linearly with increasing load. A least-square fit of Rose and Cimino's original data indicates that the wear rate is proportional to $(\text{load})^{1.41}$, which is very close to the prediction of the present theory. A previous comprehensive study by Weightman and Light [28] on the effect of surface finish of alumina and stainless steel on the wear rate of UHMWPE revealed a strong non-linear dependence on the surface roughness. A least-square fit of their original date indicates that the wear rate of UHMWPE is proportional to $R_a^{1.4}$, which is again very close to the theoretical prediction of the 1.5th power. These experimental correlations strongly support the hypotheses of the present theory.

5. Conclusion

A theoretical model has been developed to account for the microscopic wear process that occurs in UHMWPE acetabular cups. The model, which is based on a criterion of critical strain, predicts a similar correlation between wear rate and mechanical properties to the well-known Ratner–Lancaster correlation. This model is validated by the experimental results.

A transition from a microscopic surface wear to a macroscopic subsurface wear may occur under high-stress non-conformal contact conditions. The macroscopic subsurface wear or delamination may be modelled by a low-cycle fatigue process. The occurance of such a transition is strongly affected by the ultimate tensile strength and breaking elongation for the UHMWPE.

Appendix A: Nomenclature

a projected indentation radius of asperity contact
A_s true contact area swept by asperities per cycle
h average asperity height
l_o linear distance of sliding per cycle
N total number of contact asperities at any given moment
N_o total number of non-overlapping contact spots on the softer counterface per cycle
N_p total number of wear particles produced per cycle
n_c critical number of asperity contacts to produce a wear particle
P applied load
p_o mean contact pressure within each unit asperity contact spot
r average tip radius of asperities
R_a center-line-average roughness of the harder counterface
ΔV volumetric wear rate
$\delta\epsilon$ incremental plastic strain built into each unit contact spot per asperity pass
ϵ_c critical strain to produce a wear particle under a specific wear condition
ϵ_u elongation-to-failure of UHMWPE
ρ_y flow stress of UHMWPE
σ_u ultimate tensile strength of UHMWPE

References

[1] S.R. Goldring, A. Schiller, M. Roelke, C.M. Rourke, D.A. O'Neill and W.H. Harris, *J. Bone Joint Surg., 65-A* (1983) 575–584.
[2] J.H. Dumbleton, *J. Biomater. Appl. 3* (1988) 3–32.
[3] M. Jasty, C.R. Bragdon, K.R. Lee, A.E. Hanson and D.D. Goetz, *39th Ann. Meet., Orthopaedic Res. Soc., San Francisco, CA, February 15–18, 1993*, The Orthopaedic Research Society, Chicago, IL, 1993, p. 291.
[4] G.W. Blunn, A.B. Joshi, P.A. Lilley, E. Engelbrecht, L. Byd, L. Lidgren, K. Hardinge, E. Nieder and P.S. Walker, *Acta Orthop. Scand., 63* (3) (1992) 247–255.
[5] M.M. Landy and P.S. Walker, *J. Arthroplasty (Suppl), 3* (1988) S73–85.
[6] H.A. McKellop, T. Schmalzried, S.-H. Park and P. Campbell, *The 19th Ann. Meet. Soc. Biomater., April 28-May 2, 1993, Birmingham, AL*, The Society for Biomaterials, Minneapolis, 1993, p. 184.
[7] R.W. Hood, T.W. Wright and A.H. Burstein, *J. Biomed. Mater. Res., 17* (5) (1983) 829–842.
[8] D.L. Bartel, V.L. Bicknell and T.W. Wright, *J. Bone Joint Surg (Am), 68* (7) (1986) 1041–51.
[9] J.R. Cooper, D. Dowson and J. Fisher, *Wear, 162–164* (1993) 378–384.
[10] J.R. Cooper, D. Dowson and J. Fisher, *Wear 151* (1991) 391–402.
[11] T.M. Wright and D.L. Bartel, *Clinical Orthopaedics Relat. Res., 205* (1986) 67–74.
[12] W. Feller, *An Introduction to Probability Theory and Its Applications*, Vol. 1, Wiley, New York, 1968, pp. 175–190.
[13] D. Tabor, *The Hardness of Metals*, Clarendon, Oxford, 1951, pp.1–50.
[14] K.L. Johnson, *J. Mech. Phys. Solids, 18* (1970) 115.
[15] A. Wang, Ph.D Dissertation, University of Cambridge, 1988.
[16] A.E. Hollander and J.K. Lancaster, *Wear, 25* (1973) 155–170.
[17] D.C. Evans and J.K. Lancaster, *Treat. Mater. Sci. Technol., 13* (1979) 85–139.
[18] N.P. Suh, *Wear, 25* (1973) 111–124.

[19] N.P. Suh, S. Jahanmir and E.P. Abrahamson, *J. Lubr. Technol., 96* (1974) 631–637.

[20] D.A. Hills and D.W. Ashelby, *Engin. Fract. Mech., 13* (1980) 69.

[21] D. Teirlink, F. Zok, J.D. Embury and M.F. Ashby, *Acta Met., 36* (5) (1988) 1213–1228.

[22] K.L. Johnson, *Key Engin. Mater., 33* (1989) 17–34.

[23] R.W. Hertzberg and J.A. Manson, *Fatigue Engineering Plastics*, Academic Press, New York, 1980, pp. 54–61.

[24] P. Beardmore and S. Rabinowitz, in R.J. Arsenault (ed.), *Treatise on Materials Science and Technology*, Academic, New York, Vol. 6, 1975, p.267.

[25] J.G.A. Bitter, *Wear, 6* (1963) 5.

[26] J.G.A. Bitter, *Wear, 6* (1963) 169.

[27] R.M. Rose and W.R. Cimino, *Wear, 77* (1982) 89–104.

[28] B. Weightman and D. Light, *Biomater., 7* (1986) 20–24